Alves et al., J Material Sci Eng 2018, 7:5
DOI: 10.4172/2169-0022.1000494

Journal of Material Sciences & Engineering

Research Article Open Access

Dense Lamellar Scaffold as Biomimetic Materials for Reverse Engineering of Myocardial Tissue: Preparation, Characterization and Physiomechanical Properties

Alves TFR[1], Souza JF[1], Severino P[2], Andréo Filho N[3], Lima R[1], Aranha N[4,5], Silveira Filho LM[6], Rai M[7], Oliveira Junior JM[8] and Chaud MV[1]*

[1]*Laboratory of Biomaterials and Nanotechnology, University of Sorocaba, Sorocaba, ZC 18023-000, São Paulo, Brazil*
[2]*Laboratory of Nanotechnology and Nanomedicine, University of Tiradentes, Aracaju, ZC 49010-390, Sergipe, Brazil*
[3]*Laboratory of Pharmacology and Cosmetology, Federal University of São Paulo, ZC 09913-030, Diadema, São Paulo, Brazil*
[4]*Laboratory of Bioactivity Assessment and Toxicology of Nanomaterials, University of Sorocaba, Sorocaba, ZC 18023-000, São Paulo, Brazil*
[5]*Technological and Environmental Processes, University of Sorocaba, Sorocaba, ZC 18023-000, São Paulo, Brazil*
[6]*Medical Science College, State University of Campinas, Campinas, ZC 13083-887, São Paulo, Brazil*
[7]*Nanobiotechnology Laboratory, SGB Amravati University, ZC 444602, Maharashtra India*
[8]*Laboratory of the Nuclear Physical, University of Sorocaba, Sorocaba, ZC 18023-000, São Paulo, Brazil*

Abstract

The aim of this study was to develop dense lamellar scaffold as a biomimetic material for myocardial tissue regeneration. To generate dense lamellar and porous structure with biomimetic polymers was used plastic compression method. The polymeric blends of collagen, chitosan and silk fibroin were used to obtain three-dimensional devices with interconnected porous, anisotropy, and anatomical similarity with the extracellular matrix. The texture profile analysis was employed to investigate the physiomechanical properties, including mucoadhesion and swelling efficiency. Fourier transform infrared spectroscopy, differential scanning calorimetry, computerized microtomography, scanning electron microscopy were employed to investigate the structural properties, surface morphology, porosity of the dense lamellar scaffold and, cell viability and image cytometer with H9c2 cells (cardiac myoblasts). The swelling efficiency of blends was evaluated using Enslin dispositive. The physiomechanical properties associated with swelling efficiency, porosity, anisotropy degree and, cell proliferation and viability (*in vitro*) suggest that the scaffold with COL-CH-SF obtained by plastic compression may be a potential biomimetic material for reverse engineering of myocardial tissue.

Keywords: Dense lamellar scaffold; Reverse engineering; Myocardial regeneration; Collagen; Plastic compression

Introduction

Acute myocardial infarction (AMI) has been responsible for the reduction in life expectancy and large numbers of deaths worldwide. More than 17 million people die annually from cardiovascular disease, including heart attacks and strokes, according World Health Organization in 2015. The cardiovascular disease include a wide range of heart pathological condition and heart vasculature as ischemia, vascular malformation, cardiomyopathy structural, congestive heart failure and microvascular disease [1]. When occurs an AMI, the coronary artery gets occluded thus resulting in areas of hypoxia on heart. As result of AMI an inflammatory process is initiated and occurs stimulating neighboring cells to increase matrix production ultimately leading to scar tissue formation. This tissue formed is unable to contract, losing the normal pumping action, thus causing an infarct area deformed over time, myocardial remodeling and reduced cardiac output [2].

The use of regenerative medicine to treat cardiovascular disease has arisen as a research topic in the last decades. Tissue engineering products can provide one way to overcome the actually therapy limitations for cardiovascular disease, replacing the damaged myocardium by AMI or inducing constructive forms of endogenous repair, which would significantly expand patient care options [3]. Thus, tissue regeneration can be facilitated by use of biomimetic material, as biopolymers that create a suitable microenvironment for cells recruitment, adhesion, proliferation and differentiation [4].

Biomaterial is broadly defined as a material that interacts with biological systems for biomedical purposes and must be biocompatible, biodegradable, reduce local microenvironment hostility and biopersistent to facilitate cell engraftment and integration with native tissue [5,6]. The chemical composition, physiomechanical properties and 3D architecture of the scaffolds have been shown to play key roles in determining cell-microenvironment interactions and the fate of stem cells [3].

Among various biomaterials to development of the scaffolds, collagen type I are increasingly being used as protein substrates in diverse biomedical applications, because it is predominant protein in mammalian extracellular matrix [7-10]. Their main attributes include favorable fibrous structure, mechanical properties, biocompatibility, biodegradability and providing a biomimetic environment for cell growth.

Together with collagen, the chitosan and silk fibroin biomaterials have also been investigated as candidates for cardiac regeneration therapy. Was reported that mechanical strength and degradation resistance of collagen scaffold is enhanced by combining collagen with chitosan and/or silk fibroin matrixes? The addition of chitosan

***Corresponding author:** Chaud MV, Laboratory of Biomaterials and Nanotechnology, University of Sorocaba, Sorocaba, ZC 18023-000, São Paulo, Brazil, Tel: +55 15 2101-7149; E-mail: marco.chaud@prof.uniso.br

Received October 10, 2018; **Accepted** October 20, 2018; **Published** October 30, 2018

Citation: Alves TFR, Souza JF, Severino P, Andréo Filho N, Lima R, et al. (2018) Dense Lamellar Scaffold as Biomimetic Materials for Reverse Engineering of Myocardial Tissue: Preparation, Characterization and Physiomechanical Properties. J Material Sci Eng 7: 494. doi: 10.4172/2169-0022.1000494

changed the collagen fiber cross linking and reinforced the structure and porosity of the composite sponge [5,11-13].

Chitosan, a natural linear polymer obtained by chitin deacetylation, can be used as a cell scaffold or carrier for controlled and localized drug delivery. This natural material displays high biocompatibility and biodegradability, has the capacity growth factor retention and strong cellular receptor adhesion due to its hydrophilicity. When mixed with natural materials, chitosan and/or silk fibroin scaffolds acquire other properties that favor cell maturation, adhesiveness, and scaffold coupling with the host myocardium [13,14].

However, collagen hydrogel shows a large volume and occupies a significant space to use in myocardium muscle. To reduce collagen hydrogel contraction without affecting its biocompatibility, Brown et al. [15] and later others [16-19] developed a compressed collagen hydrogel technique (plastic compression) for tissue engineering through the rapid expulsion of fluid, producing scaffolds that are relatively dense and mechanically strong, with controllable mesoscale structures.

The plastic compression of collagen gels consists in transition of an initial state of a highly hydrated gel without structural competence to one of a relatively dense gel with the ability to support its own weight and provide resistance to fluid flow. During one-dimensional compression, the highly hydrated gel collapses against a rigid, porous support and forms a relatively dense gel layer (lamella) on top of this support, reminiscent of solute concentration polarization during ultrafiltration and gel formation. Therefore, at a microstructural level the highly hydrated gel transitions abruptly to a gel layer, resulting in a multi-layer model describing collagen gel compacted [20].

The present study aimed to develop and to evaluate with controllable mesoscale structures the dense lamellar scaffold as a biomimetic material for myocardial tissue regeneration. The different polymeric blends of collagen, chitosan and silk fibroin were used to obtain biomimetic three-dimensional devices, by plastic compression.

Materials and Methods

Materials

The collagen powder extracted from bovine hides, were supplied by NovaProm Food Ingredients Ltda. (São Paulo, Brazil). These samples were used without any chemical treatment. Chitosan of average molar mass, 75-85% deacetylate (Sigma-Aldrich Co, Saint Louis, USA), DMEM (Sigma-Aldrich Co, Saint Louis, USA) and cocoon of the *Bombyx mori.* The other reagents were of pharmaceutical grade.

Preparation of fibroin Solution

Bombyx mori silk fibroin was prepared adapted from Komatsu et al. [21]. Briefly, silk sericin was extracted by treating silk cocoons in an aqueous solution of 0.5 wt% Na_2CO_3 (120°C) for 15 min using an autoclave. The silk fibroin was rinsed thoroughly with water to extract the sericin proteins. The degummed silk fibroin was dissolved in $CaCl_2.2H_2O/CH_3CH_2OH/H_2O$ solution (mole ratio, 1:2:6) at 85°C. Then the fibroin solution (SF) was filtered and dialyzed against distilled water for 3 days to yield SF. The final fibroin concentration was about 2–3 wt%, which was determined by weighing the remaining solid after drying.

Preparation of chitosan hydrogel

The chitosan (CH) of average molar mass was used to prepare the hydrogel. Briefly, 3.0 g of the CH was added into 100 mL of the glacial acetic acid solution (1.5% v/v) and shaken until complete dissolution.

Preparation of collagen-chitosan hydrogel

The collagen dispersion was prepared by addition of 2 mL DMEM (Sigma, MO, US), 0.75 g or 1 g of collagen type I and, water enough to obtain 10 mL of dispersion. The COL and CH hydrogels were mixed in the rate of 9:1 (m/m) and this hydrogel was used to prepare the COL-CH scaffold. The dispersions were placed into cylindrical containers (inner diameter=21 mm and height=11 mm), and incubated at 10°C for 24 h for polymerization.

Preparation of collagen-chitosan-fibroin hydrogel

The collagen dispersion was prepared by addition of 2 mL DMEM (Sigma, MO, US), 0.75 g or 1 g of collagen type I and, water enough to obtain 10 mL of dispersion. The COL, CH an SF hydrogels were mixed in the rate of 9:1:5 (m/m/v) and this hydrogel was used to prepare the COL-CH-SF scaffold. The dispersions were placed into cylindrical containers (inner diameter=21 mm and height=11 mm), and incubated at 10°C for 24 h for polymerization.

Preparation of dense lamellar scaffolds

Dense lamellar scaffolds for AMI were produced by plastic compression (using hydrostatic press), adapted from Brown et al. Briefly, cast highly hydrated hydrogels were transferred to a porous support comprising (bottom to top) absorbent paper blot layers, a steel mesh and two nylon meshes. Subsequently, a static compressive stress of 4 KN was applied to the hydrated scaffolds for 10 min in order to remove water and produce a dense biomaterial with improved biological and mechanical properties. Finally, the matrices were freeze-dried, resulting in cross-linked collagen-chitosan scaffolds.

Physiomechanical and mucoadhesive properties

Texture profile analysis (TPA) was using to measure the physiomechanical properties (elasticity, flexibility, drilling and resistance to traction) of scaffolds were performed using a Stable Micro Systems texture analyzer (Model TA-XT Plus) in texture profile analysis mode with load cell of 5 Kg. The samples (approximately 40 mm diameter) were hydrated for 1 h or 7 days, excess of the water was removed, and after were fixed in suitable apparatus with hole. Test velocity was defined for rate of 2 $mm.s^{-1}$ for drilling and resistance to traction test and 0.5 mm. s^{-1} for elasticity and flexibility test. Elastic (Young's) modulus was obtained by compressed until densification occurred, at which point the tests were stopped (strain ranged approximately between 0 and 5%).

The mucoadhesive properties of scaffolds were evaluated using a Stable Micro Systems texture analyzer (Model TA-XT Plus). Mucin discs were prepared for compression (Lemaq, Mini Express LM-D8, Diadema, Brazil), using flat punches, cylindrical matrix with a diameter of 8 mm and a compression load of 8 tons. The mucin discs showed diameter of 8 mm and thickness of 0.2 mm and, were previously hydrated and fixed to the lower end of the analytical probe. The samples (41 mm diameter) were fixed in suitable apparatus with hole. Mucin disc fixed in the probe was compressed on the surface of the scaffold with a force of 0.098 N, directed in the apical → basal. Contact time between mucin disc and sample was of 100 s, stipulated for an intimate contact of the mucin disc with the sample. The probe was removed of the scaffold surface with constant quickness of 10 $mm.s^{-1}$. The force required to detach the mucin disc from the surface of scaffold was determined from the time (s) × force (g) ratio.

Swelling efficiency

The swelling efficiency profile was obtained by Enslin dipositive [22]. Briefly, the samples were kept in touch with buffer solution pH 7.4 by 16 hours. To perform this study were used samples with 1 cm^2, and were put onto the sintering filter and the volume of media absorbed by the sample after predetermined times was measured with the graduated pipette of the device. The volume of liquid absorbed by the sample was noted and graphically plotted (volume of liquid absorbed × time).

Porosity, interconnectivity and pore size

The morphometric characteristic of the porosity, interconnectivity and pore size of scaffolds were evaluated by computerized microtomography (μCT). The scaffolds pictures were captured by X-Ray microtomograph (Brucker-micro CT - SkyScan 1174, Kontich, Belgium) with high resolution scanner (28 mM pixel and integration time at 1.7 s). The source of the X-rays was 34 keV of energy and 790 mA of current. The projections were acquired in a range of 180° with an angular step of 1° of rotation. 3D virtual models representative of various regions of scaffolds were created and the data were mathematically treated by CT Analyzer v. 1.13.5.

Scanning electron microscopy (SEM)

SEM photographs scaffolds were obtained using a scanning electron microscope (LEO Electron Microscopy/Oxford, Leo 440i, Cambridge, England) with a 10 kV accelerating voltage. All samples were affixed to a brass specimen holder using double-sided adhesive tape, and the powders were made electrically conductive by coating with gold using a sputter-coater for 4 min at 15 mA.

Differential scanning calorimetry (DSC)

DSC was performed on a Shimadzu, TA-60, Kyoto, Japan, calibrated using indium as the reference material. A sample of 2 mg was packed in a hermetically crimped aluminum pan, and heated under dry nitrogen purged at 30 $mL.min^{-1}$. The samples were heated from 25 to 340°C at a rate of 5°C min^{-1}.

Fourier transform infrared spectroscopy (FTIR)

FTIR analysis (Shimadzu, IRAffinity-1, Kyoto, Japan) was used to collect FT-IR spectra via Labs Solutions Software v.2.10. The chemical functionalities of the samples were determined by an attenuated total reflectance (ATR) cell on the FTIR spectrophotometer over the range between 4000 and 600 cm^{-1} at 4 cm^{-1} resolutions, averaging 128 scans.

Cell viability - mitochondrial activity assay (MTT)

The cellular analyses were evaluated just for COL-CH-SF scaffolds, based on the best results presented in the other analyses. In order to evaluate cell viability, the material was initially extracted and kept in the culture medium for 24 hours. The extract was made using a 1 cm^2 fragment in 2.5 mL culture medium. This concentration of material is equivalent to exposing 1.6 m of material to a 70 kg individual.

Approximately 5 × 10^5 cells/well (H9c2 cells - cardiac myoblasts) were plated in 96-well plates, after 24 h period and total cell adhesion treatments were performed using the extracts at 100, 50 and 25% dilutions, and were maintained for a period of 24 h. After the treatment, the culture medium was removed and 100 μl of MTT solution (3-(4,5-dimethylthiazolyl-2)-2,5-diphenyltetrazolium bromide) at 5 mg/ml was added to each well. After 3 hours in the oven at 37°C, the MTT solution was withdrawn and 100 μl of DMSO per well was added for cell attachment. The reading was performed using ELISA microplate reader at 570 nm.

Image cytometer

Initially (Time 0 h) 1 × 10^5 cells/well (H9c2 cells - cardiac myoblasts) were plated in a 24 well plate, which was incubated at 37°C-5% CO_2 using Minimum Essential Alpha medium with ribonucleosides, deoxyribonucleosides, 2 mM L-glutamine and 1 mM sodium pyruvate, without ascorbic acid plus fetal bovine serum to a final concentration of 10%. After 24 hours and total adhesion of the cells, they were placed in contact with the material for 48 and 72 hours. After the treatment period, the samples were removed from the cultures and the cells were washed with PBS, trypsinized and counted using the Image Cytometry technique.

Results

The mesoscale analysis of the scaffold obtained by plastic compression showed stable and uniform physical structure and absence of the furrow, indicating that the process used was capable of getting the scaffold (Figure 1). Thus, the crosslinking has been confirmed to play an important role related to the scaffold with porous structure distribution and with the ability of water containing [23]. The plastic compression was an efficient technique to get the dense lamellar scaffold, based on collagen, with potential use for cardiac regeneration by reverse engineering (Figure 1).

Physiomechanical and mucoadhesive properties

Figure 2 shows the mechanical resistance results of the scaffold obtained by plastic compression after 1 hour and after 7 days. When the scaffolds were hydrated for

1 hour the drilling, tensile strength and mucoadhesion properties of the scaffolds containing COL and CH showed better results than scaffold with SF ($p<0.05$), however the elasticity (Table 1) and flexibility properties (Figure 2) were the same for both formulations with and without SF (COL-CH and COL-CH-SF). After 7 days of the hydration the COL-CH scaffolds showed decrease for all mechanical properties studied ($p<0.05$), this fact can be assigned to relaxation of the polymers chains and the kind of crosslinking formed (Figure 2).

After 7 days the scaffolds containing SF (COL-CH-SF), showed

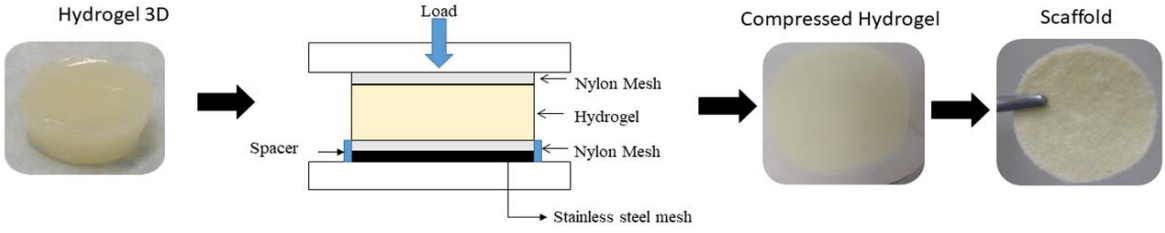

Figure 1: Dense lamellar scaffold obtained by plastic compression.

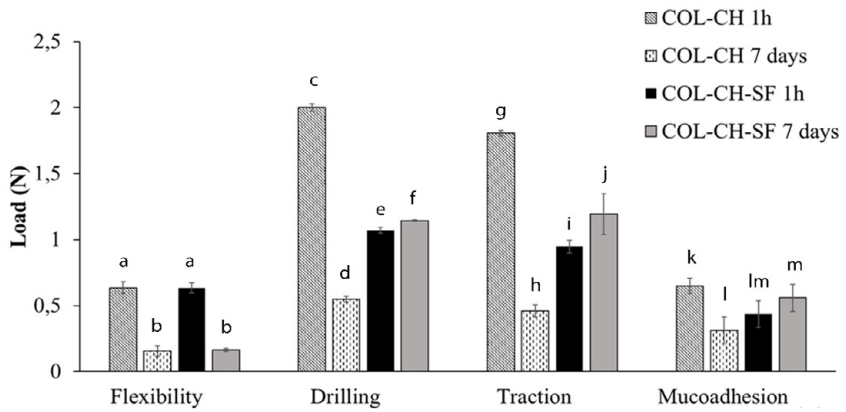

Figure 2: Physiomechanical properties of dense lamellar scaffolds. Equal letters (for the same analysis) indicate that there is no significant difference between the mean values (p>0.05) (n=3).

	1 hour Elasticity (KPa)	7 days Elasticity (KPa)
COL-CH	0.726 ± 0.089	1,697.746 ± 87.416
COL-CH-SF	0.784 ±0.058	2,022.034 ± 144.019

Table 1: Mechanical properties of Young's modulus of scaffolds (after 1 hour and 7 days in aqueous medium).

decrease for flexibility properties and increase for tensile strength ($p<0.05$). Although, the drilling and mucoadhesion properties were kept ($p>0.05$). The results obtained with Young's modulus (Table 1) revealed that the introduction of SF to COL-CH significantly increases the values of this parameter for COL-CH-SF (2,022.034 ± 144.019 kPa) scaffolds compared with COL-CH (1,697.746 ± 87.416 kPa) (Table 1).

Thus, our results showed that SF increases significantly the Young's modulus of COL-CH scaffolds after 1 h (1,697.746 ± 87.416 KPa) and 7 days (2,022.034 ±144.019 KPa) of water immersion.

Swelling efficiency

Figure 3 shows the volume of buffer absorbed (mL) by the sample in function of time (h). The results show that hydrophilic equilibrium of the scaffolds COL-CH and COL-QT-SF after 16 hours was not yet reached, since the curve profile is upward. Until 12 hours the profiles were similar and statically equals ($p>0.05$), after than the COL-CH scaffold showed a volume of liquid absorbed greater than the absorbed by COL-CH-SF ($p<0.05$). The end of scaffold of COL-CH profile indicates that the hydrophilic equilibrium will be reached because a baseline is starting after 15 hours. However, after 15 hours was observed that COL-CH-SF scaffold shows the upward profile.

For both scaffolds were observed anomalous transport, when the n values were 0.79 and 0.88, respectively to COL-CH and COL-CH-SF.

Porosity, interconnectivity and pore size

The morphological and morphometric characteristic of dense lamellar scaffolds are showed in Table 2, Figures 4 and 5. The COL-CH and COL-CH-SF scaffolds had the regular interconnected structure with large porosity (Table 2). The pores interconnectivity of the COL-CH and COL-CH-SF scaffolds were 71.68% and 79.01%, respectively. The pores were oriented with rounded shape in both formulations (Figures 4 and 5). The values obtained to degrees of anisotropy of the COL-CH and COL-CH-SF scaffolds were 0.426 and 0.4, respectively.

Figure 5 shows SEM images of compacted and freeze–dried scaffolds prepared from collagen/chitosan and collagen/chitosan/

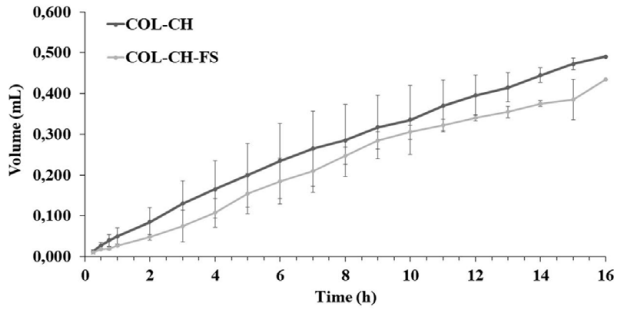

Figure 3: Swelling efficiency profile of dense lamellar scaffolds.

	COL-CH	COL-CH-SF
Pore interconnectivity (%)	71.68	79.01
Volume of open pores (mm^{-3})	2.66	2.14
Closed porosity (%)	0.15	0.2
Degree of anisotropy	0.426	0.400

Table 2: Morphological characteristics of scaffolds.

fibroin blend. The pores size for COL-CH-SF scaffold were 10x bigger than COL-CH scaffold.

Differential scanning calorimetry (DSC)

Figure 6A and 6B show the thermogram of polymers and scaffold COL-CH, and COL-CH-SF. The first thermic events between 45 and 110°C (Figure 6) are associated with lose of the water from the excipients and scaffolds formulations. In the Figure 6 (panel A-SF) the endothermic peak at 281°C is related as a thermal degradation of SF. To CH thermogram Figure 6 (panel A) the thermal event at 302°C is an exothermic peak it may be related to the decomposition of amine (GlcN) units [24].

A denaturation temperature (Td) of COL-CH scaffold was recorded at 67.2°C whereas COL-CH-FS exhibited Td peak at 68.6°C [25]. A single glass-transition temperatures (Tg's) occurred at 220°C to COL-CH and COL-CH-SF scaffolds, the same was observed for COL in the natural form.

Fourier transform infrared spectroscopy (FTIR)

Infrared spectra show stretches characteristic of COL, CH, SF

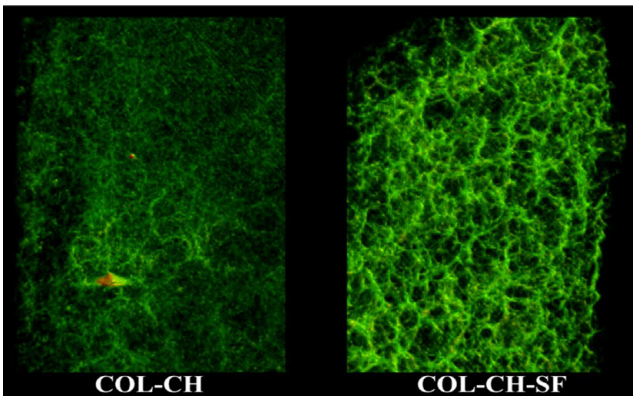

Figure 4: Morphometric characteristic of dense lamellar scaffolds evaluated by computerized microtomography.

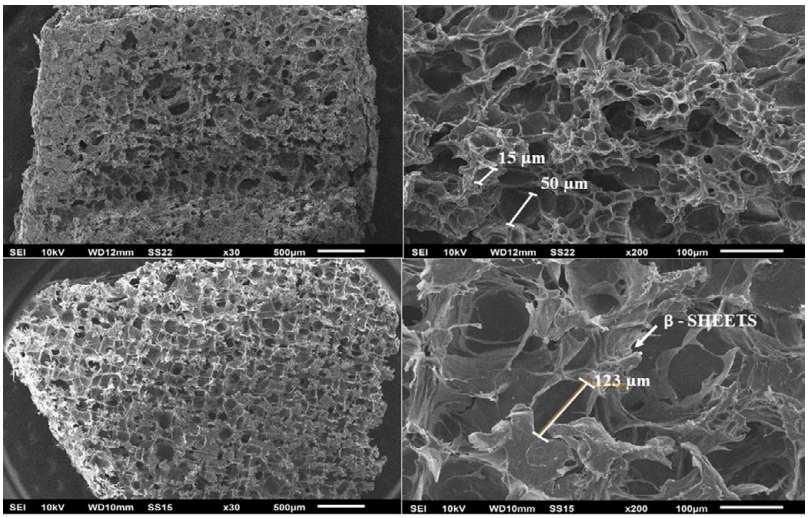

Figure 5: Scanning electron microscopy of dense lamellar scaffolds.

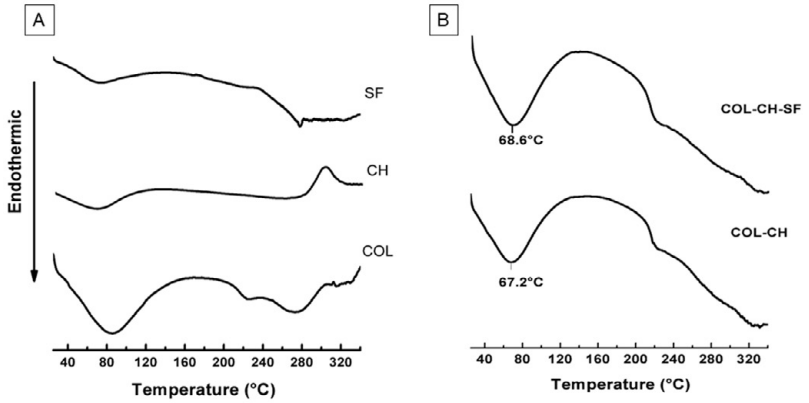

Figure 6: Differential scanning calorimetry of COL, CH, SF (panel A), and scaffolds samples (panel B).

(Figure 7A) and scaffolds samples (Figure 7B). The spectrum of collagen depicts characteristic absorption bands in 1645 cm^{-1} corresponding to amide I absorption arises predominantly from protein amide C=O stretching vibrations and 1546 cm^{-1} corresponding to amide II is made up of amide N-H bending vibrations and C-N stretching vibrations. The 1240 cm^{-1} corresponding to amide III band is complex, consisting of components from C-N stretching and N-H in plane bending from amide linkages. The peaks identified at 1454 cm^{-1} and in the region between 1417 cm^{-1} and 1360 cm^{-1} correspond to the stereochemistry of the pyrrolidine rings of proline and hydroxyproline. Additionally,

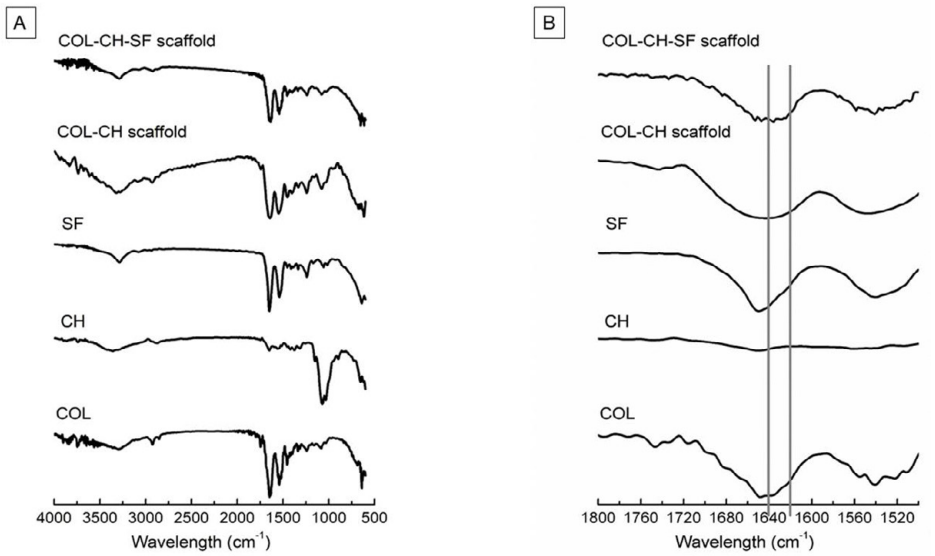

Figure 7: Infrared spectra of COL, CH, SF (panel A) and scaffolds samples (panel B).

bands at 3450, 2850 and 1450 cm^{-1} were observed, which represent the stretching of -OH, -CH_3 and pyrrolidine rings, respectively.

The spectrum of chitosan depicts characteristic absorption bands at 3352, 2878 cm^{-1}, attributed to the -OH and -CH_3 groups. Furthermore, bands were identified at 1560 and 1404 cm^{-1} typical of the N-H group bending vibration and vibrations of -OH group of the primary alcoholic group, respectively. The bands at 1320 and 1077 cm^{-1} correspond to the stretching of C-O-N and C-O groups. The bands at 1154 and 897 cm^{-1} are attributed to the glycosidic bonds. The shoulder at 1650 cm^{-1} represents the stretching of C=O.

Pure SF shows absorption bands at 1645 cm^{-1} (amide I) and 1546 cm^{-1} (amide II), corresponding to the SF silk II structural conformation (β-sheet). Other absorption bands were observed at 1530 cm^{-1} (amide II) and 1236 cm^{-1} (amide III), which are characteristic of the silk I conformation (random coil and α-helix) this results were compatible with literature.

The FTIR spectra of the COL-CH and COL-CH-SF scaffolds show the characteristic bands of the parent molecules, indicating that did not have chemical interaction between the polymers used in the formulation.

Cell viability - Mitochondrial activity assay (MTT)

The results are showed in Figure 8 and show the cellular viability after 24 hours of scaffold exposure. According to our results, no significant differences between control group and COL-CH-SF scaffolds. The viability for scaffold was greater than 90%. It is not possible in these concentrations to determine the IC_{50}.

Image cytometer

The results show that COL-CH-SF scaffold presents a significant difference during growth with respect to the control, after 48 and 72 hours, presenting a decrease of cellular multiplication (Figure 9).

Discussion

To construct a scaffold in heart tissue engineering with biomimetics characteristics, it is need to consider the critical factors as thickness, pore size range, mechanical strength, biodegradability, swelling

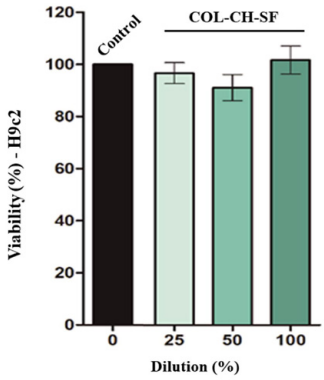

Figure 8: Results of MTT analyses, exposure to control and COL-CH-SF scaffold in H9c2 cells for 24 h.

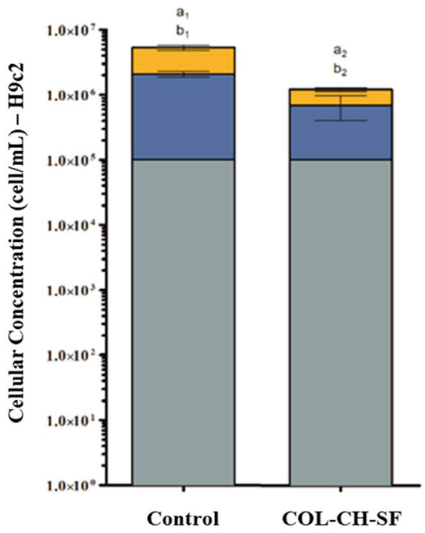

Figure 9: Results regarding cell growth (H9c2) after exposure to COL-CH-SF.

capacity and biopersistence. Cell adhesion is a fundamental process directly involved in cell growth, cell migration, and cell differentiation. The surface hydrophilicity, the presence of ionic charges parameters and chemical composition influence these interactions [11].

The gel formation with the blend of polymers (COL, CH and SF) was induced by pH correction, this factor was important to improve the crosslinking and to provid a 3D formation [9]. However, the collagen gels show a poor mechanical properties when pre-compressed due the excess of the fluid present in untreated collagen. The development of the plastic compression (PC) technique can rapidly produce dense, mechanically strong collagen scaffolds with controllable microscale features and biomimetic function [26,27].

Dense collagen scaffolds mimicking the ECM fibrillar density and microstructure which have great potential for tissue engineering applications, such as skin grafts, cornea epithelial reconstructs, myocardium and bone regeneration [28].

Physiomechanical and Mucoadhesive Properties

The myocardium is a muscle highly elastic, and elastic relaxation during diastole is essential for proper heart function. The elastic modulus of the scaffold and elastic deformation is a critical characteristic to the myocardium. Myocardial tissue has the stiffness of the left ventricle ranges from 10-20 kPa during diastole and 200–500 kPa during systole [29,30]. Therefore, the scaffolds should be able to maintain its shape and be mechanically robust to withstand the contraction and relaxation straight. The microstructure and stiffness properties affect the bioactivity, migration and adhesion of cells into the scaffolds. Thus, the characterization of the stiffness of the 3D tissue-engineered scaffold can allow the effect of this parameter on cell activity in a more realistic situation [8,31,32].

The mechanical properties of 3D scaffold are elasticity, flexibility, drilling and tensile. The elastic modulus or Young's modulus of the material (i.e. stiffness) is the ability of the scaffold to return to its original form after deformation, which is a critical characteristic of the myocardium tissue. Young's modulus is commonly used to try and quantify an intrinsic elastic property of soft, viscoelastic biomaterials [29]. The flexibility of scaffolds is related with the capacity of material to suffer a maximum external deformation without to fracture the crosslinking of the polymers. The drilling of scaffolds is the force at the maximum distance of a compression cycle or the maximum force reached prior to a fracture. The tensile strength is the measure of the force or stress required to stretch the scaffold (resistance to lengthwise stress) to the point where it breaks or before permanent result of deformation.

Mucoadhesion can be defined as the bond produced by contact between the scaffold and the mucin that recovers the membrane surface. The mucus is an external layer of gel-like material secreted by goblet cells, compound of the water, inorganic salts, lipids, and mucins, highly glycosylated glycoproteins with many cysteine residues on their backbone structure [33].

The dense lamellar scaffolds obtained by our group have not used crosslinking agent as glutaraldehyde, carbodiimide, epoxy compounds, acyl azide or any natural crosslinking agent. After 7 days of the hydration the COL-CH scaffolds showed decrease for all mechanical properties studied ($p<0.05$), this fact can be assigned to relaxation of the polymers chains and the kind of crosslinking formed. In collagen, the -OH groups of hydroxyproline are involved in hydrogen bonds between chains, while interactions between other side groups are thought to be important in the formation of fibrils. These side groups are capable of forming hydrogen bonds with -OH and $-NH_2$ groups in chitosan. Moreover, the end group -COOH and $-NH_2$ in collagen-may also form hydrogen bonds with -OH and $-NH_2$ groups from chitosan, as chitosan possesses large numbers of -OH groups. Additionally, COL-CH may be bonded ionically. These molecules are capable of forming complexes with oppositely charged ionic polymers, particularly the cationic polysaccharide chitosan and anionic -COOH group in collagen [34].

The results obtained with Young's modulus (Table 1) revealed that the introduction of SF to COL-CH significantly increases the values of this parameter for scaffolds compared with COL-CH. Cheema and Brown, and Hadjipanayi et al. produced the collagen scaffolds by the same technique of plastic compression. The results obtained by themselves in Young's modulus test were similar to our found [27,35]. Serpooshan et al. produced collagen scaffolds by plastic compression technique using different compression load. They obtained scaffolds with Young's modulus (stiffness) between 0.34 and 1.4 KPa [3].

These studies have been performed to check the relation between stiffness of material and the cell proliferation. The results demonstrated the preferential accumulation of cells towards the stiffer regions of the gradient [35-37]. If we compare our results with those obtained by Serpooshan et al. we can assert based on Young's modulus, that the COL-CH-SF scaffolds have an environment more favorable to cell proliferation than those obtained by them.

Silk fibroin is composing by silks I and silks II. The silks I provides a good water solubility since is formed by α-helix and β-sheet. The silks II is the main structural configuration of the SF and is rich in β-sheet, it provides a poor water solubility. The high resistance to water permeation decrease the scaffold dissolution time. SF has reactive carboxyl groups and amino groups in its side chains, it can react with other functional groups being able to keep or to improve the mechanical properties of scaffolds, even after 7 days immersed in aqueous environment [38]. Gobin et al. assigns this behavior is due to increased regions of β-sheets, which increase the amount of crystalline domains and increase tensile strength and stiffness. Sun et al. produced COL-SF scaffolds and observed that after 14 days immersed of culture medium, the thickness and Young's modulus of the scaffolds increased [39].

Water molecules from the environment migrate to the microscopic pores or voids in the compound to achieve concentration equilibrium. The moisture mass obtained by a polymer occurs in two states, mobile or bound. The first state is sometimes called physical absorption by polymers based on Fick's laws. The second state is when the water molecules become chemically bonded to the polymer chain' hydroxyl groups. This chemical absorption process can be irreversible and causes non-Fickian behavior [40].

By determining the diffusional exponent, n, one can gain information about the physical mechanism controlling solute uptake by or drug release from a particular device. For a film, n=0.5 indicates Fickian diffusion, $n > 0.5$ indicates anomalous transport and n=1 implies case II (relaxation-controlled) transport [41]. Since most polymers swell when they are in contact with certain solvents, one can use Fick's laws with modified boundary conditions and/or a generalized diffusion coefficient to address the non-Fickian behavior [42].

The swelling efficiency test (Figure 3) indicated that the water-binding ability of the COL-CH or COL-CH-SF scaffolds could be attributed to both of their hydrophilicity and the maintenance of their three-dimensional structure. In general, the swelling ratio is decreased

with the increases crosslinking degree due the decrease of the free hydrophilic groups. For both scaffolds were observed anomalous transport, when the n values were 0.79 and 0.88, respectively to COL-CH and COL-CH-SF. The anomalous transport is observed when the diffusion and relaxation rates are comparable and govern the moisture absorption.

The scaffolds properties to cardiac regeneration should have an interconnected porous structure, high porosity, and appropriate pore dimensions to favor cell homing and migration, cellular anchorage, vascularization, and oxygen, nutrient, metabolite diffusion. These factors must be considered and balanced with the understanding of the well-known effect of stiffness on cellular differentiation. A three-dimensional scaffolds which were prepared by plastic compression and lyophilization had porous structure confirmed by μCT (Figure 4) and SEM (Figure 5).

The major limitation of the conventionally fabricated cardiac scaffolds is their isotropic nature. The tissue that is formed into the pores of an isotropic scaffold is a negative or mirror image of the scaffold itself, and since most tissue has anisotropic arranged extracellular matrix components and concomitant mechanical properties, the tissue formed has no structural and mechanical relationship with the native tissue. Anisotropic scaffolds with a porous, tubular or other structure, that enable direct differentiation into the native tissue configuration might be extremely helpful to realize this goal. The anisotropy is associated with lamellar characteristic on scaffolds. The use of μCT allows to obtain the degrees of anisotropy of the scaffolds (Table 2), that can range from 0 (structure is completely isotropic) to 1 (structure is completely anisotropic) [43,44]. The values obtained to degrees of anisotropy of the COL-CH and COL-CH-SF scaffolds were 0.426 and 0.4, respectively. Thus, the scaffolds produced are partially lamellar (anisotropic). The result of degree anisotropy added up to mechanical (Figure 2 and Table 1) and structural (Table 2 and Figures 4 and 5) properties are suitable to stimulate the cell growth, the tissue formation and to withstand the stiffness of the left ventricle (10-20 kPa during diastole and 200-500 kPa during systole) [29].

The SEM images are according to LV et al. [45], it is common the sheets formation in structure surface of the scaffold when the same is added of fibroin. This information corroborates with our SEM results (Figure 5C and 5D) obtained for COL-CH-SF scaffold. The analyze of results presented in Figure 2 show that the drilling and traction properties increased with hydration time.

Thermal degradation peaks of SF films at temperatures in the 290°C region are characteristic of amorphous SF (silk I) and are present when SF films are not submitted to any kind of physical or chemical treatment to induce its conformation to a more stable structure (silk II) [46]. Thermal decomposition peaks of collagen observed between 220-350°C also were observed by Shanmugasundaram et al. León-Mancilla et al. related that endothermic peak at 325°C could be due the loss of hydrogen bonds, so this phenomenon of protein denaturation, could be initiated in this interval of temperature which the tertiary structure is lost. Although, this phenomenon is reversible if the protein is newly hydrated.

Triple helix of collagen are held together by hydrogen bonds and crosslinking stabilizes the triple helical structure of collagen by forming intramolecular and intermolecular network The DSC thermogram of COL-CH and COL-CH-FS are shown in Figure 6A and 6B). DSC is used to measure the denaturation temperature (Td) which is a measure of crosslinking density. It gives a better understanding of unfolding of protein under the influence of temperature. The DSC plots gives an endothermic peak associated with helix to coil transition which indicates the extent of intermolecular crosslinking.

In general, the miscibility of the polymers blend depends on the self-association and inter-association of hydrogen-bonding donor polymers. This miscibility can be analyzed with DSC to determine when has a single glass-transition temperature (Tg's) [47-49]. The Tg's at 220°C to COL-CH and COL-CH-SF scaffolds can be also observed for COL in the natural form, indicating that COL, CH and SF form a miscible blend.

FTIR is commonly used to investigate the conformation of SF and blend of COL-CH-SF. The FTIR spectra represent typical absorption bands sensitive to the molecular conformation of SF. The FTIR in the range of 1800-1500 cm^{-1} (Figure 7B) was analyzed to investigate the β-sheet formation (1640-1620 cm^{-1}) [50] in the COL-CH-SF scaffolds. The analyze of spectra showed that was displacement of the band related to random coil conformation (1650-1640 cm^{-1}) for conformation β-sheet (1640-1620 cm^{-1}). This fact indicates that the scaffold manufacturing process and/or blend of polymers are able to convert random coil to β -sheet conformation. The FTIR spectra of scaffold shows that did not have chemical interaction between the polymers used in the formulation.

Cell viability and proliferation was widely assayed by the MTT, which was a quantitative colorimetric assay. The purple crystals can be formed by metabolically active cells and was detected by spectrophotometry at 520 nm. So, growth and proliferation of active cells can be tested indirectly using this method [51]. To confirm the cell viability and proliferation was made the image cytometer. In general, it is possible to observe that the material leads to an initial imbalance in the cells tested, but these seem to return to normal after a period of 72 h, as observed in Figure 9, where there are differences of the exposed material in relation to the control (without exposure). As no significant cell death was observed on exposure, it is concluded that the material does not lead to cell death but an initial decrease in multiplication that is restored after the 72 h period.

Conclusion

The plastic compression is an efficient technique to produce the dense lamellar scaffold with physiomechanical properties to be evaluated in reverse engineering of myocardial tissue. The characterization by FTIR shows the transition of random coil to β-sheet conformation, which positively influence the physiomechanical properties and swelling efficiency of dense lamellar scaffold, composed of collagen, chitosan and silk fibroin. The images captured by μCT and SEM show that scaffold has the regular interconnected structure with large porous and high anisotropy degree. So, the COL-CH-SF scaffold may be an ideal biomimetic template for reverse myocardial tissue engineering. Considering the obtained result in this study, we observed that the selection of the biomaterial as scaffold does not influence cell proliferation and viability significantly *in vitro* condition.

References

1. Taylor DA, Sampaio LC, Gobin A (2014) Building new hearts: A review of trends in cardiac tissue engineering. Am J Transplant 14: 2448-2459.
2. Domenech M, Polo-Corrales L, Ramirez-Vick JE, Freytes DO (2016) Tissue Engineering Strategies for Myocardial Regeneration: Acellular Versus Cellular Scaffolds? Tissue Eng Part B Rev 22: 438-458.
3. Serpooshan V, Zhao M, Metzler SA, Wei K, Shah PB, et al. (2013) The effect of bioengineered acellular collagen patch on cardiac remodeling and ventricular function post myocardial infarction. Biomaterials 34: 9048-9055.

4. O'Brien FJ (2011) Biomaterials & scaffolds for tissue engineering. Mater. Today 14: 88-95.
5. Cui Z, Yang B, Li RK (2016) Application of Biomaterials in Cardiac Repair and Regeneration. Engineering 2: 141-148.
6. Lam MT, Wu JC (2012) Biomaterial applications in cardiovascular tissue repair and regeneration. Expert Rev Cardiovasc Ther 10: 1039-1049.
7. Generali M, Dijkman PE, Hoerstrup SP (2014) Bioresorbable Scaffolds for Cardiovascular Tissue Engineering. EMJ Interv Cardiol 1: 91-99.
8. Sargeant TD, Desai AP, Banerjee S, Agawu A, Stopek JB (2012) An in situ forming collagen-PEG hydrogel for tissue regeneration. Acta Biomater 8: 124-132.
9. Maximo GJ, Cunha RL (2010) Mechanical Properties of collagen fiber and powder gels. Journal of Texture Studies 41: 842-862.
10. Venkatesan J, Jayakumar R, Anil S, Chalisserry EP, Pallela R, et al. (2015) Development of Alginate-Chitosan-Collagen Based Hydrogels for Tissue Engineering. J Biomater Tissue Eng 5: 458-464.
11. Kim SE, Cho YW, Kang EJ, Kwon IC, Lee EB, et al. (2001) Three- dimensional porous collagen/chitosan complex sponge for tissue engineering. Fibers Polym 2: 64-70.
12. Arpornmaeklong P, Pripatnanont P, Suwatwirote N (2008) Properties of chitosan-collagen sponges and osteogenic differentiation of rat-bone-marrow stromal cells. Int J Oral Maxillofac Surg 37: 357-366.
13. She Z, Zhang B, Jin C, Feng Q, Xu Y (2008) Preparation and in vitro degradation of porous three-dimensional silk fibroin/chitosan scaffold. Polym Degrad Stab 93: 1316-1322.
14. Perea-Gil I, Prat-Vidal C, Bayes-Genis A (2015) In vivo experience with natural scaffolds for myocardial infarction: the times they are a-changin. Stem Cell Res Ther 6: 248.
15. Brown RA, Wiseman M, Chuo CB, Cheema U, Nazhat SN (2005) Ultrarapid engineering of biomimetic materials and tissues: Fabrication of nano- and microstructures by plastic compression. Adv Funct Mater 15: 1762-1770.
16. Hu K, Shi H, Zhu J, Deng D, Zhou G, et al. (2010) Compressed collagen gel as the scaffold for skin engineering. Biomed Microdevices 12: 627-635.
17. Serpooshan V, Quinn TM, Muja N, Nazhat SN (2013) Hydraulic permeability of multilayered collagen gel scaffolds under plastic compression-induced unidirectional fluid flow. Acta Biomater 9: 4673-4680.
18. Buxton PG, Bitar M, Gellynck K, Parkar M, Brown RA, et al. (2008) Dense collagen matrix accelerates osteogenic differentiation and rescues the apoptotic response to MMP inhibition. Bone 43: 377-385.
19. Busby GA, Grant MH, MacKay SP, Riches PE (2013) Confined compression of collagen hydrogels. J Biomech 46: 837-840.
20. Serpooshan V, Quinn TM, Muja N, Nazhat SN (2011). Characterization and modelling of a dense lamella formed during self-compression of fibrillar collagen gels: implications for biomimetic scaffolds. Soft Matter 7: 2918.
21. Komatsu D, Aranha N, Chaud MV, Júnior JM de O, Mistura DV, et al. (2017) Characterization of Membrane of Poly (L,co-D,L-lactic acid-co-trimethylene carbonate) (PLDLA-co-TMC) (50/50) loaded with Silk Fibroin. SDRP J Biomed Eng 2: 1-11.
22. Fahr A, Voigt R (2000) Pharmazeutische technologie: für Studium und Beruf. (9th ed) Stuttgart.
23. Wang HM, Chou YT, Wen ZH, Wang ZR, Chen CH, Ho ML (2013) Novel Biodegradable Porous Scaffold Applied to Skin Regeneration. PLoS One 8: 2-12.
24. Guinesi LS, Cavalheiro ÉTG (2006) The use of DSC curves to determine the acetylation degree of chitin/chitosan samples. Thermochim. Acta 444: 128-133.
25. Lakra R, Kiran MS, Usha R, Mohan R, Sundaresan R, Korrapati PS (2014) Enhanced stabilization of collagen by furfural. Int J Biol Macromol 65: 252-257.
26. Mi S, Chen B, Wright B, Connon CJ (2010) Plastic compression of a collagen gel forms a much improved scaffold for ocular surface tissue engineering over conventional collagen gels. J. Biomed. Mater. Res. - Part A 95 A: 447-453.
27. Cheema U, Brown RA (2013) Rapid Fabrication of Living Tissue Models by Collagen Plastic Compression: Understanding Three-Dimensional Cell Matrix Repair In Vitro. Adv. Wound Care 2: 176-184.
28. Xia Z, Villa MM, Wei M (2015) A Biomimetic Collagen-Apatite Scaffold with a Multi-Level Lamellar Structure for Bone Tissue Engineering. J Mater Chem B Mater Biol Med 14: 1998-2007.
29. Kaiser NJ, Coulombe KLK (2015) Physiologically inspired cardiac scaffolds for tailored in vivo function and heart regeneration. Biomed Mater 10: 034003.
30. Radisic M, Christman KL (2013) Materials science and tissue engineering: Repairing the heart. Mayo Clin Proc 88: 884-898.
31. Davidenko N, Campbell JJ, Thian ES, Watson CJ, Cameron RE (2010) Collagen-hyaluronic acid scaffolds for adipose tissue engineering. Acta Biomater 6: 3957-3968.
32. Chaud M V, Alves TFR, Rebelo MA, Souza JF de, Amaral VA, Barros CT, et al. (2017) Three-Dimensional and Biomimetic Technology in Cardiac Injury After Myocardial Infarction: Effect of Acellular Devices on Ventricular Function and Cardiac Remodelling. In: Scaffolds in Tissue Engineering - Materials, Technologies and Clinical Applications pp: 227-251.
33. Eshel-Green T, Eliyahu S, Avidan-Shlomovich S, Bianco-Peled H (2016) PEGDA hydrogels as a replacement for animal tissues in mucoadhesion testing. Int. J. Pharm 506: 25-34.
34. Sionkowska A (2004) Molecular interactions in collagen and chitosan blends. Biomaterials 25: 795-801.
35. Hadjipanayi E, Mudera V, Brown RA (2009) Guiding cell migration in 3D: A collagen matrix with graded directional stiffness. Cell Motil. Cytoskeleton 66: 121-128.
36. Gangaraju Vamsi K. Lin Haifan (2009) Cell adaptation to a physiologically relevant ECM mimic with different viscoelastic properties. Nat Rev Mol Cell Biol 10: 116-125.
37. Hadjizadeh A, Doillon CJ (2010) Close dependence of fibroblast proliferation on collagen scaffold matrix stiffness. J Tissue Eng Regen Med 4: 524-531.
38. Li ZH, Ji SC, Wang YZ, Shen XC, Liang H (2013) Silk fibroin-based scaffolds for tissue engineering. Frontiers of Materials Science 7: 237-247.
39. Sun K, Li R, Jiang W, Sun Y, Li H (2016) Comparison of three-dimensional printing and vacuum freeze-dried techniques for fabricating composite scaffolds. Biochem. Biophys. Res. Commun 477: 1085-1091.
40. Placette MD, Fan X, Edwards D (2011) A dual stage model of anomalous moisture diffusion and desorption in epoxy mold compounds. 12th Intl. Conf. Therm. Mech. Multi-Physics Simul. Exp. Microelectron. Microsystems.
41. Ganji F, Vasheghani-Farahani S, Vasheghani-Farahani E (2010) Theoretical Description of Hydrogel Swelling: A Review. Iran Polym J 19: 375-398.
42. Rossi G, Mazich KA (1993) Macroscopic description of the kinetics of swelling for a cross-linked elastomer or a gel. Phys. Rev. E 48: 1182-1191.
43. Mulder ELW, Buma P, Hannink G (2009) Anisotropic porous biodegradable scaffolds for musculoskeletal tissue engineering. Materials (Basel) 2: 1674-1696.
44. Silva AMH da, Alves JM, Silva OL da, Silva Junior NF (2014) Two and three- dimensional morphometric analysis of trabecular bone using X-ray microtomography (μCT). Rev. Bras. Eng. Biomédica 30: 93-101.
45. Lv Q, Feng Q, Hu K, Cui F (2005) Three-dimensional fibroin/collagen scaffolds derived from aqueous solution and the use for HepG2 culture. Polymer (Guildf) 46: 12662-12669.
46. Freddi G., Pessina G., Tsukada M (1999) Swelling and dissolution of silk fibroin (Bombyx mori) in N-methylmorpholine N-oxide. Int J Biol Macromol 24: 251.
47. Shanmugasundaram N, Ravichandran P, Reddy PN, Ramamurty N, Pal S, Rao KP (2001) Collagen- chitosan polymeric scaffolds for the in vitro culture of human epidermoid carcinoma cells. In Vitro 22: 1943-1951.
48. León-Mancilla BH, Araiza-Téllez MA, Flores-Flores JO, Piña-Barba MC (2016) Physico-chemical characterization of collagen scaffolds for tissue engineering. J Appl Res Technol 14: 77-85.
49. Kuo SW, Huang CF, Chang FC (2001) Study of Hydrogen-Bonding Strength in Poly (ε-caprolactone) Blends by DSC and FTIR. 39: 1348-1359.
50. Sionkowska A, Płanecka A (2013) Preparation and characterization of silk fibroin/chitosan composite sponges for tissue engineering. J Mol Liq 178: 5-14.
51. Sun K, Li H, Li R, Nian Z, Li D, Xu C (2014) Silk fibroin/collagen and silk fibroin/chitosan blended three-dimensional scaffolds for tissue engineering. Eur J Orthop Surg Traumatol 25: 243-249.